

Modified methods of stellar magnetic field measurements

A. F. Kholtygin^{1,*}

Astronomical Institute of Saint-Petersburg University, Russia

Received 2012, accepted 2012

Published online later

Key words stars: magnetic fields – methods: analytical

The standard methods of the magnetic field measurement, based on an analysis of the relation between the Stokes V -parameter and the first derivative of the total line profile intensity, were modified by applying a linear integral operator \hat{L} to the both sides of this relation. As the operator \hat{L} , the operator of the wavelet transform with DOG-wavelets is used. The key advantage of the proposed method is an effective suppression of the noise contribution to the line profile and the Stokes parameter V . The efficiency of the method has been studied using the model line profiles with various noise contributions. To test the proposed method, the spectropolarimetric observations of the A0-type star α^2 CVn, young O-type star θ^1 Ori C and A0 supergiant HD 92207 were used. The longitudinal magnetic field strengths for these stars calculated by our method appeared to be in a good agreement with those determined by other methods.

© 2011 WILEY-VCH Verlag GmbH & Co. KGaA, Weinheim

1 Introduction

Measurements of stellar magnetic fields are based mainly on polarization observations. In 1947 Babcock detected for the first time the dipole stellar magnetic field of 78 Vir with the surface polar field of about 1500 G (Babcock 1947). Since that time different methods of stellar magnetic field measurements were developed. These methods were used for measuring the magnetic fields of about thousand stars of various spectral types from young T Tau and Herbig Ae/Be stars to red giants (Bychkov et al. 2009).

Methods of the magnetic field measurements are mainly based on the determination of the value of the displacement $\overline{\Delta\lambda_B}$ between left (L) and right (R) circular polarized Zeeman components of spectral lines in a presence of the magnetic field. Direct measurements of the value of $\overline{\Delta\lambda_B}$ are possible mostly in the case of spectra with sharp lines or for strong fields with magnetic induction B larger than 1 kG and also for best quality spectra with signal-to-noise ratio $S/N \geq 1000$. Such good quality spectra can be obtained mainly for the brightest stars. Detection of the magnetic field of the early-type stars with wide spectral lines and moderate values of the magnetic field in a few hundred gauss seems to be very difficult.

To increase the effective S/N a multiline technique is usually used to extract the information from many spectral lines. The multiline technique is most effective for stars with a large number of lines in their spectra. For example, for A and late type stars weak magnetic fields B of about 1 G can be detected with 3σ confidence (Petit et al. 2010).

At the same time, for early-type OB and Wolf-Rayet (WR) stars with broad lines in their spectra, the measurement of moderate magnetic fields $B \leq 100$ G presents a very serious problem. Moreover, the wider lines in the stellar spectra are the less effective are the measurements of a magnetic field of the star. This means that for different types of stars various methods of the magnetic field measurements have to be used.

An analysis of the signal in the Stokes parameter V is ordinary used to measure the magnetic fields. The ratio of the Stokes parameter within the spectral line, $V(\lambda)$, to the line profile intensity $I(\lambda)$ in the unpolarized spectrum, can be presented as (see, e.g., Landstreet, 1982, Hubrig et al. 2006):

$$\frac{V(\lambda)}{I(\lambda)} = -\overline{\Delta\lambda_B} \frac{1}{I(\lambda)} \frac{dI(\lambda)}{d\lambda} = -\mathcal{K}_0 g_{\text{eff}} \lambda_0^2 \langle B_l \rangle \frac{1}{I(\lambda)} \frac{dI(\lambda)}{d\lambda}. \quad (1)$$

where g_{eff} is the effective Landé factor for the line, $\langle B_l \rangle$ is the mean longitudinal magnetic field, λ_0 is the central wavelength for the line, the coefficient $\mathcal{K}_0 = e/4\pi m_e c^2 = 4.6686 \cdot 10^{-13} [\text{\AA}^{-1} \text{G}^{-1}]$. Here e is the electron charge, m_e is the mass of the electron and c is the speed of light.

Based on Eq. (1) two approaches, differential and integral ones are used to measure the stellar magnetic field. In the first approach the value of $\langle B_l \rangle$ is determined as a coefficient of the linear regression for Eq. (1). This regression method was described in detail by Bagnulo et al. (2002). In the paper by Bagnulo et al. (2006) the estimations of the $\langle B_l \rangle$ errors for the regression method are given.

Hereinafter we will call the differential approach as differential method (DM) of the magnetic field measurement. The first line profile derivative $dI/d\lambda$ is calculated numerically (see, for example, Eq. (4) in the paper by Bagnulo et al.

* A. F. Kholtygin: e-mail: afkholtygin@gmail.com

2006), that leads to large errors in its value due to noise contribution in the line profile (e.g., Hubrig et al. 2006). Generally a large number of spectral lines have to be used in the DM to reach a better accuracy.

In the integral approach (integral method, IM) the first moments from the left and right sides of Eq. (1) are calculated. For convenience, instead of the wavelength λ , the Doppler velocity shift from the line center $w = (\lambda - \lambda_0)/c$, is used, where λ_0 is the central wavelength of the line. Then

$$\alpha_1(V) = \int_{-\Delta w}^{\Delta w} wV(w)dw = -\mathcal{R}_0\lambda_0g_{\text{eff}}\langle B_l \rangle \int_{-\Delta w}^{\Delta w} [I_c - I(w)] dw . \quad (2)$$

Here $\alpha_1(V)$ is the first moment of the Stokes parameter V , I_c is the intensity of the continuum, $I(w)$ is the continuum normalized intensity for velocity w . The value of Δw can be taken as about of 2-3 of the line FWHM. The coefficient $\mathcal{R}_0 = 1.3996 \cdot 10^{-7} [\text{km/s} \text{ \AA}^{-1} \text{ G}^{-1}]$. Integral $W_{\text{line}} = \int_{-\Delta w}^{\Delta w} [I_c - I(w)] dw$ is the equivalent width of the line in km/s. It should be noted that the DM is typically used for spectra with unresolved spectral lines, while the IM is used for spectra with resolved spectral lines.

Using the moments of the line profiles of different orders in integral light and the Stokes parameter V allows us to determine not only the mean longitudinal magnetic field $\langle B_l \rangle$ but also the field crossover and the mean quadratic magnetic field (Mathys, 1995, Mathys & Hubrig, 1997).

Semel (1989) and Semel & Li (1996) used the multiline technique to reach the best accuracy of the magnetic field measurements. They proposed a plain averaging of the polarization measurements of many spectral lines to detect and analyze magnetic fields (*line addition*) method.

Donati et al. (1997) improved the line co-addition procedure and had introduced the least-squares deconvolution (LSD) method. This method assumes that all spectral lines can be described by a scaled basic line profile. They also proposed that overlapping lines add up linearly. These assumptions led to a simplified description of the intensity and circular polarization observations in terms of the convolution of the known line mask with an unknown line profile. The approximation is used to reconstruct the average line shape and the LSD profile of the Stokes parameter V . Kochukhov et al. (2010) extended the LSD approach to the analysis of circular and linear polarization in the spectral lines for the case when the shape of lines can be described by different functions. Alternative multiline Zeeman signature was introduced by Semel et al. (2009) and Ramirez Velez et al. (2010). They have used the line addition technique to show how to extract a Zeeman signature for any of the Stokes parameters. These techniques, apart from being applicable to any state of polarization, are model independent.

For an effective realization of different methods of the magnetic field measurements, the polarimetric spectra with a rather high S/N and with large number of lines in their spectra are usually required. However, application of the above mentioned methods to OB and WR stars displaying smaller number of very broad spectral lines is not simple (e.g., Kholtygin et al. 2011b).

On the other hand, it is well known, that smoothing the line profiles with different filters allows one to suppress the noise contribution in the line profiles and to reveal the weak line profile details (Kholtygin et al. 2003, Kholtygin et al. 2006). We suggest in this work that a certain kind of smoothing of the Stokes parameter V enables one to achieve a larger efficiency of the various multiline methods for the magnetic field determination in upper main-sequence stars and lets us to detect the magnetic fields for stars with wide and noisy line profiles.

The modification of the standard procedures of the magnetic field measurements is described in the present paper. It is based on the application of the linear integral transforms to both sides of Eq. (1) or Eq. (2). The transform with the DOG wavelet is used to smooth the Stokes parameter V and line profile derivative. The proposed approach was partly outlined by Kholtygin et al. (2011a).

Our paper is organized as follows. In Sect. 2 we present the main relations and basic assumptions. The different presentations of the linear integral transform of the Stokes parameter V is considered. We examine the application of the proposed method for the analysis of the arbitrary number of lines and spectra in Sect. 3. In this section the method is also tested for the different kinds of model line profiles. The application of the method to the archival observations is outlined in Sect. 4. In the last section we summarize the main results.

2 Mathematical basis of the proposed methods

2.1 Main relations

A profile of an arbitrary line in the stellar spectra as a function of a Doppler displacement w can be presented as:

$$I(w) = I_c + \mathcal{Z}(w) + \mathcal{N}(w). \quad (3)$$

Here I_c has the same meaning as in Eq. (2), $\mathcal{Z}(w)$ is a function describing the net line profile and $\mathcal{N}(w)$ is the noise contribution. Hereafter we assume that the net line profile $\mathcal{Z}(w)$ is stable over the time of observations and the amplitude of the noise component is determined by the noise of the detector.

Similarly, the profiles of (L) and (R) polarized components of the line are determined by the formulas:

$$\begin{cases} I_L(w) = I_c^L + Z_L(w) + \mathcal{N}_L(w), \\ I_R(w) = I_c^R + Z_R(w) + \mathcal{N}_R(w), \end{cases} \quad (4)$$

where symbols have the same meaning as in Eq. (3), but for left-hand (L) and right-hand (R) polarized components

separately. The line profiles are assumed to be normalized at the continuum level. For the continuum normalized spectra $I_c = I_L^c = I_R^c = 1$.

As a next step, we suppose that the noise components $\mathcal{N}_L(w)$ and $\mathcal{N}_R(w)$ are the independent random values. The splitting $\overline{\Delta w_B}$ of the line in the Doppler velocities space is

$$\overline{\Delta w_B} = \mathcal{R}_0 g_{\text{eff}} \lambda_0 \langle B_l \rangle \quad [\text{km/s}], \quad (5)$$

With the line intensities $I_L(w)$ and $I_R(w)$ for (L) and (R) polarized components the Stokes parameter V and the total line intensity I

$$\begin{cases} V(w) = \frac{1}{2} [I_L(w) - I_R(w)] , \\ I(w) = \frac{1}{2} [I_L(w) + I_R(w)] . \end{cases} \quad (6)$$

For the small value of $\overline{\Delta w_B}$, analogously to Eq. (1), we can write

$$\begin{aligned} V(w) &= -\overline{\Delta w_B} \frac{dI(w)}{dw} = \\ &= -\mathcal{R}_0 g_{\text{eff}} \lambda_0 \langle B_l \rangle \frac{dI(w)}{dw}. \end{aligned} \quad (7)$$

Eqs. (5)-(7) are valid exactly only for local line profiles. In the simplest field configurations as the oblique rotator model there is the simple connection between the $\langle B_l \rangle$ and the polar field strength (Preston 1967). In the case of more complicated field configurations the connection between the value of $\langle B_l \rangle$ and the global stellar surface magnetic field distribution is not evident. The analysis of the longtime series of Stokes IQUV profiles and some kind of the Magnetic Doppler Imaging technique (e.g., Kochukhov-2004) can be used to restore this distribution.

2.2 Linear transform of the Stokes parameter V

For OB stars with typical values of $\langle B_l \rangle = 100 - 300$ G the line shift $\overline{\Delta w_B}$ is very small, and for noisy line profiles the derivative dI/dw is calculated with large errors. For this reason Eq. (7) should be modified to obtain the more reasonable estimation of the extremely small difference between (L) and (R) components. Applying the operator \hat{L} of the arbitrary linear integral transform to the left and right sides of Eq. (7) we obtain:

$$V_L(w) = \hat{L} [V(w)] = \langle B_l \rangle J_L(w), \quad (8)$$

where $V_L(w)$ is the Stokes parameter $V(w)$, which is smoothed using the operator \hat{L} and the integral

$$J_L(w) = -\mathcal{R}_0 g_{\text{eff}} \lambda_0 \hat{L} \left[\frac{dI(w)}{dw} \right], \quad (9)$$

Using Eq. (4) and neglecting the terms which are proportional to a small value $\overline{\Delta w_B}^2$ we find

$$\begin{aligned} J_L(w) &= -\mathcal{R}_0 g_{\text{eff}} \lambda_0 \left(\hat{L} \left[\frac{dZ(w)}{dw} \right] \right. \\ &\quad \left. + \frac{1}{2} \hat{L} \left[\mathcal{N}_L(w) + \mathcal{N}_R(w) \right] \right). \end{aligned} \quad (10)$$

The main advantage of the proposed procedure lies in a possibility to provide an effective suppression of the noise contribution in the line profile. If we use a suitable form of the linear operator \hat{L} then the value of the noise component $\hat{L} [\mathcal{N}_L(w) + \mathcal{N}_R(w)]$ becomes smaller. It allows us to improve the accuracy of the magnetic field determination.

2.3 Smoothing the Stokes parameter V with Gaussian filter of a variable width

As a possible form of the operator \hat{L} we will consider a set of operators \hat{L}_G^k of the convolution of the source function $f(x)$ with the family of functions $\mathcal{G}_k(x/S)$ having a variable width S , where

$$\mathcal{G}_k(x) = \frac{(-1)^k}{\sqrt{2\pi}} \frac{d^k}{dx^k} \left[\exp \left(-\frac{x^2}{2} \right) \right]. \quad (11)$$

with $k = 0, 1, 2, \dots$. Coefficients in Eq. (11) are selected in such a manner that at $k = 0$ the function $\mathcal{G}_0(x)$ is the unbiased Gaussian function with a width $S = 1$. At $k \geq 1$ the function $\mathcal{G}_k(x)$ is proportional to DOG-wavelet $\psi_k(x)$ with an index k (e.g., De Moortel et al. 2004).

With different values of the index k one can construct the various approaches to measure the mean longitudinal magnetic field $\langle B_l \rangle$. In the present paper we consider only the simplest case $k = 0$. Applying the operator \hat{L}_G^0 to the left and right sides of equation (7) we obtain:

$$\begin{aligned} V(w, S) &= \frac{1}{\sqrt{2\pi}} \times \\ &\int_{-\infty}^{\infty} e^{-\frac{1}{2} \left(\frac{w-x}{S} \right)^2} V(x) dx = \langle B_l \rangle J(w, S), \end{aligned} \quad (12)$$

where

$$\begin{aligned} J(w, S) &= \frac{\mathcal{R}_0 g_{\text{eff}} \lambda_0}{S^2 \sqrt{2\pi}} \times \\ &\int_{-\infty}^{\infty} (w-x) e^{-\frac{1}{2} \left(\frac{w-x}{S} \right)^2} \left[I(x) - I_c \right] dx. \end{aligned} \quad (13)$$

A value of $V(w, S)$ in Eq (12) is the Stokes parameter V , which is smoothed with the Gaussian filter of the variable width S , while the function $J(w, S)$ in Eq (13) is proportional to the wavelet transform of the net line profile $[I(x) - I_c]$ with the WAVE wavelet $(2\pi)^{-1/2} x \exp(-x^2/2)$ and the scaling parameter S . Hereafter we will use Eq. (12) to determine the value of the magnetic field $\langle B_l \rangle$.

2.4 Modified differential and integral methods of the field determination

In the modified differential method (MDM) we use directly Eq. (12). The value of $\langle B_l \rangle$ is derived by the least squares method as linear fitting of $V(w, S)$ vs. $J(w, S)$.

The modified integral method (MIM) is also based on Eq. (12). Multiplying the left and right sides of this relation by the Doppler velocity shift w and integrating over the line profile we obtain:

$$\begin{aligned} M_V &= \int_{-\Delta w}^{\Delta w} w V(w, S) dw = \\ \langle B_l \rangle &\int_{-\Delta w}^{\Delta w} w J(w, S) dw = \langle B_l \rangle M_J. \end{aligned} \quad (14)$$

Here M_V and M_J are the first moments of the Stokes parameter V and the parameter J , respectively. The limits of integration $-\Delta w$ and Δw in Eq. (19) are the same as in Eq. (2). Eq. (14) is used to find the value of $\langle B_l \rangle$ by the integral method. Results of our calculations show that the differences between the values of $\langle B_l \rangle$ obtained using both MDM and MIM in most cases are not very significant.

2.5 Testing the method for the single line model profiles

To test the method we use the model profiles of L and R components of line calculated for a fixed input model field B_{inp} . The normalized Gaussian profile for the shape of the spectral lines is used:

$$\begin{cases} I_L^{\text{mod}}(w) = I_c + Z_0 e^{-\frac{1}{2} \left(\frac{w - \overline{\Delta w_B}}{\sigma_w} \right)^2} + N(0, s_N), \\ I_R^{\text{mod}}(w) = I_c + Z_0 e^{-\frac{1}{2} \left(\frac{w + \overline{\Delta w_B}}{\sigma_w} \right)^2} + N(0, s_N), \end{cases} \quad (15)$$

where Z_0 is the line depth at $\lambda = \lambda_0$. The value of $\overline{\Delta w_B}$ is determined by Eq. (5), and σ_w is the width of the model profile in km/s. $N(0, s_N)$ is the normally distributed random value with zero mathematical expectation and the standard deviation $s_N = (S/N)^{-1}$, where S/N is the signal-to-noise ratio in the spectral region where the considered line is located.

The unsmoothed model profile of the Stokes parameter V for the line He I $\lambda 4921.9$ with parameters $Z_0 = -0.35$, $\sigma_w = 80$ km/s and spectral resolving power $R = 60000$ for different S/N values is given in Fig. 1 (top panel) for the illustration. The smoothed Stokes parameter $V(w, S)$ strongly depends on the S/N (Fig. 1, middle panel). In the bottom panel in Fig. 1 the parameter $J(w, S)$ for the same signal-to-noise ratios is given. It is evident that although at $S/N = 50$ the noise contribution strongly distorts the line profile and the Stokes parameter V , the value of $J(w, S)$ remains practically unchanged. The calculations show that for all scales S in the interval of 10 km/s $\leq S \leq 160$ km/s the parameter J weakly depends on the S/N .

Let us to apply the MDM to the model profile of the line He I $\lambda 4921$ for the input value of $B_{\text{inp}} = 400$ G and $S/N = 800$. Approximating the dependence of the smoothed parameter $V(w, S)$ on $J(w, S)$ at the filter width $S = 80$ km/s and using the standard formulas of the least-squares method (e.g., Brandt 1970), we obtain $\langle B_l \rangle = 398 \pm 18$ G (see Fig. 2, top panel) in a good agreement with input field value. Here the value of $\sigma_{\text{fit}} = 18$ G is the error of the of least-squares method approximation. In order to reach the best fit, the contribution of the line wings is ignored when the net line intensity is close to the noise level. In the top panel the standard error of the smooth Stokes parameter $V(w, S)$ is plotted. The errors of the parameter $J(w, S)$ are too small (about of 0.01%) to be drawn.

Results of applying both the MDM and the MIM methods for the magnetic field determination depend on the value of scaling parameter S . Below we discuss how to choose the

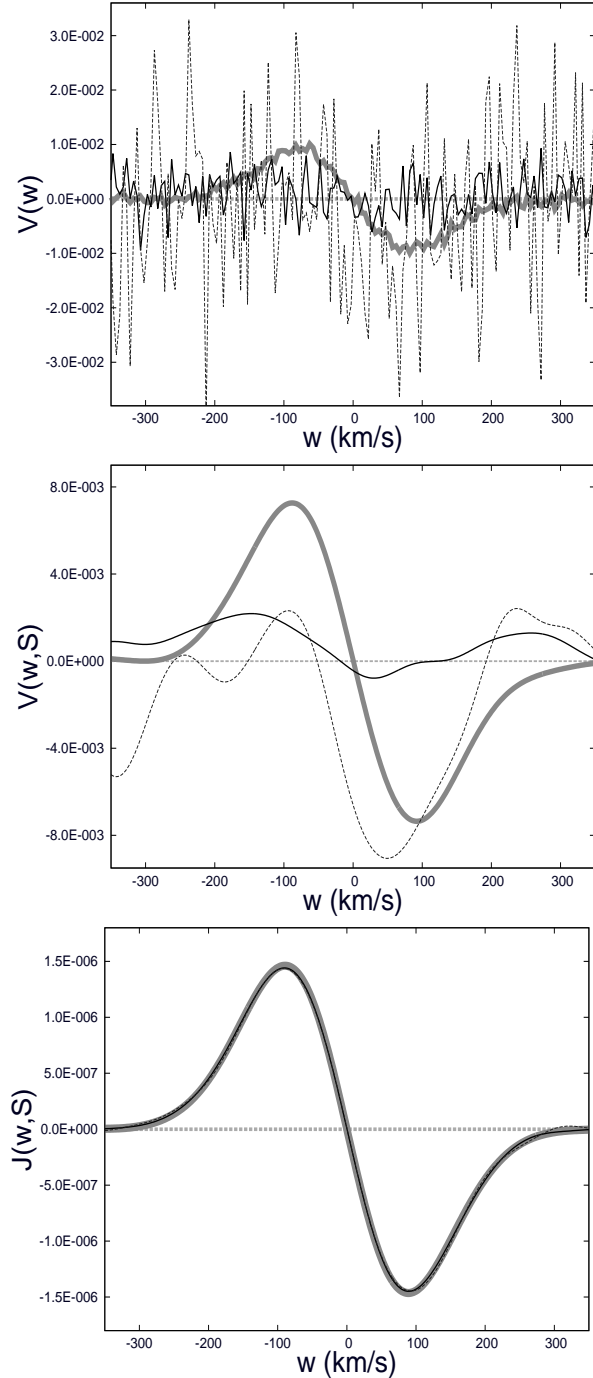


Fig. 1 Top panel: the unsmoothed Stokes parameter $V(w)$ for the line He I $\lambda 4921.9$ with parameters $Z_0 = -0.35$, $\sigma_w = 80$ km/s. Thick grey solid line corresponds to $S/N = 1000$, thin solid line comply with $S/N = 200$, while dashed one corresponds to $S/N = 50$. Middle Panel: the smoothed Stokes parameter $V(w, S)$, where the filter width $S = 40$ km/s for $S/N = 1000$ (thick grey solid line), $S/N = 1000$ (thin solid line) and $S/N = 50$ (dashed line). Bottom panel: the same as in the middle panel but for the parameter $J(w, S)$.

optimal value of S . Suppose that we vary the scaling parameter S for some fixed line profile. Then, the optimal value of S corresponds to the minimum of the absolute value of

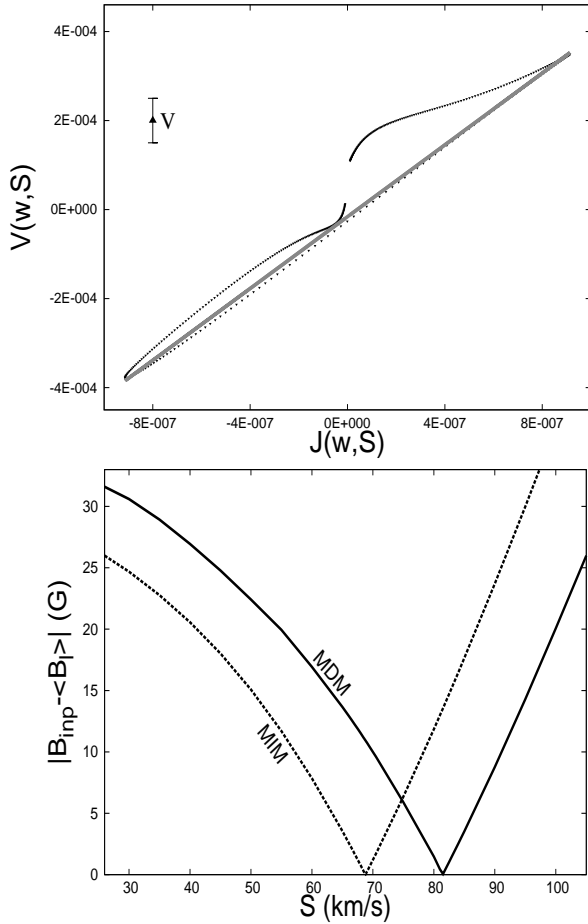


Fig. 2 Top panel: dependence of Eq. (12) of the smoothed Stokes parameter $V(w, S)$ vs. $J(w, S)$ for model profile of the He I λ 4921 at the scale $S = 80$ km/s (filled triangles) and the value of $B_{\text{inp}} = 400$ G. Grey solid line shows the linear regression line for this dependence. The standard error of the parameter $V(w, S)$ is given. Bottom panel: the absolute values of the difference $|B_{\text{inp}} - \langle B_l \rangle|$ for the MDM (solid line) and the MIM (dashed line).

the difference $|B_{\text{inp}} - \langle B_l \rangle|$ between input field B_{inp} and its fitted value $\langle B_l \rangle$. In Fig. 2 (bottom panel) this difference is plotted for the MDM (solid line) and the MIM (dashed line). We see that the optimal value $S_{\text{opt}} \approx 81$ km/s for the MDM, while $S_{\text{opt}} \approx 69$ km/s for the MIM.

It means that $S_{\text{opt}} \approx 0.4$ FWHM both for the MDM and the MIM. Moreover, the minimum of the fit error σ_{fit} for the MDM is achieved at $S = 78$ km/s, which is close to values of S_{opt} both for the MDM and the MIM. These relations between S_{opt} and FWHM are also held for other parameters of the model line profiles. The following procedure can be proposed to select the optimal value of the scale S . Firstly, we vary the parameter S in the interval $[0.3, 0.5]$ of FWHM. Secondly, we are looking for the value of the scale S , which gives us the minimal error of the least-square fit of the $V(w, S)$ vs. $J(w, S)$ dependence. And finally, we choose this value of the scale S as its optimal value. Here-

inafter this algorithm of the optimal value of S selection is used.

It has to be noted that the value of σ_{fit} is not the error of the value of $\langle B_l \rangle$ itself as it is often proposed. These errors describe the measure of the inaccuracy of the linear fit of the smoothed parameter $V(w, S)$ vs. $J(w, S)$ dependence only. The real error σ_B of $\langle B_l \rangle$ can be determined by the methods described in the next section. For the He I λ 4921 Å line profile with parameters given above it gives $\sigma_B = 115$ G. This value is much larger than σ_{fit} .

It is worth noting that the integration in Eq. (14) is numerical and its accuracy depends on a number of points of the integration n_{int} in the line profile. This number in turn is determined by the spectral resolving power R and mean profile width V_{line} in the velocity space. For stars with profiles broadened by rotation, the value $V_{\text{line}} \approx 2V \sin i$.

For the numerical integrations the trapezoidal method is used. Our calculations show that the accuracy of integration weakly depend on the chosen numerical technique.

To be certain that the magnetic field determined by the MIM is realistic, the condition $n_{\text{int}} \geq 6$ has to be performed. For the spectral resolving power R the step in the wavelengths is about $\Delta\lambda = \lambda_0/R$, where λ_0 is the central wavelengths of the line and the corresponding value in the velocity space is $\Delta w = c/R$. Assuming that $n_{\text{int}} > 6$ we can find the minimal width of the line profile in the velocity space, which can provide the necessary accuracy of the magnetic field determination, $V_{\text{line}} \geq n_{\text{int}} c/R$.

It means that the MIM is most efficient for stars with wide line profiles, e.g. fast rotating OB and WR stars. As for the MDM, this limitation for the line profile width is not important and this method can be applied to stars with both wide and narrow lines.

2.6 Distribution of measured values of the magnetic field

As it was pointed out above, the least-squares fit of the dependence of $V(w, S)$ vs. $J(w, S)$ can underestimate the error σ_B of the measured value of $\langle B_l \rangle$. The real value of σ_B can be only obtained if we know the distribution function of the measured $\langle B_l \rangle$ values. The measured value of $\langle B_l \rangle$, which is determined from the analysis of the line splitting, is the random value. It depends on the random contribution of the noise component in the line profile for given spectropolarimetric observation. Each new observation, even for the fixed values of S/N , the fixed resolving power R and other fixed parameters of the set of the observations, gives its own value of $\langle B_l \rangle$. To obtain the real probability distribution for $\langle B_l \rangle$ we need the extremely huge number of observations. Happily we can estimate the distribution function using the model line profiles.

First, we fix the parameters $Z_0, \sigma_w, g_{\text{eff}}$ of the model profiles and also parameters S/N and R , which determine the quality of the set of observations. Second, we simulate a

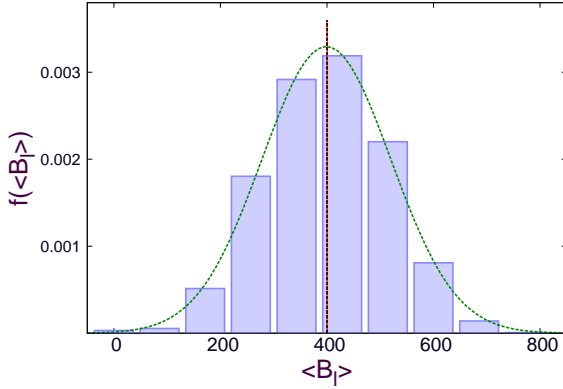


Fig. 3 The distribution function $f(\langle B_l \rangle)$ of the values $\langle B_l \rangle$, which is determined from the analysis of the model HeI λ 4921.9 line profiles with parameters $R = 60000$, $S/N = 800$, $B_{\text{inp}} = 400$ G, $Z_0 = -0.35$, $\sigma_w = 80$ km/s and the scaling parameter $S = 80$ km/s. The approximation of $f(\langle B_l \rangle)$ by the Gaussian is drawn by a dashed line. A vertical dashed line marks the input value of $B_{\text{inp}} = 400$ G.

large number $N_{\text{sp}} \gg 1$ of the model profiles with fixed values of S/N and R and random noise contribution. Third, we calculate the values of $\langle B_l \rangle$ for all N_{sp} model line profiles. And finally we divide the whole range of the calculated values of $\langle B_l \rangle$ for the random noise component into intervals with the width of $\Delta \langle B_l \rangle$. The probability distribution function $f(\langle B_l \rangle)$ can be found from the following relation:

$$f(\langle B_l \rangle + \Delta \langle B_l \rangle / 2) = \frac{N(\langle B_l \rangle, \langle B_l \rangle + \Delta \langle B_l \rangle)}{N_{\text{sp}} \Delta \langle B_l \rangle}, \quad (16)$$

where $N(\langle B_l \rangle, \langle B_l \rangle + \Delta \langle B_l \rangle)$ is the number of the field measurements, which gives the value of $\langle B_l \rangle$ in the interval $[\langle B_l \rangle, \langle B_l \rangle + \Delta \langle B_l \rangle]$.

Table 1 The mean longitudinal magnetic field strengths $\langle B_l \rangle$ and the corresponding errors σ_B obtained for different input field strengths (B_{inp}) using the MDM and the MIM. The value of the scale parameter $S = 50$ km/s.

B_{inp}, G	MDM		the MIM	
	$\langle B_l \rangle, \text{G}$	σ_B, G	$\langle B_l \rangle, \text{G}$	σ_B, G
250	236	67	266	95
500	493	69	499	83
1000	1016	61	1014	95
1500	1507	63	1504	97
2000	2013	73	2022	99

In Fig. 3 we present the distribution function $f(\langle B_l \rangle)$ obtained by the above described method for the input value of $B_{\text{inp}} = 400$ G from the analysis of the model profiles of the HeI λ 4921.93 line for value of $N_{\text{sp}} = 10^4$. Inspecting this figure we can conclude that the mathematical expectation of the measured field value $M(\langle B_l \rangle) \approx B_{\text{inp}}$, while the standard deviation $\sigma_B \approx 120$ G.

For an illustration of the efficiency of the MDM and the MIM we present in Table 1 the average values of the mean longitudinal magnetic field $\langle B_l \rangle$, which are determined by the MDM and the MIM from the analysis of the model profiles of the HeI λ 4921.93 line using the numerical experiment described in the previous paragraphs. All model profiles are calculated for different input values of the magnetic field B_{inp} and fixed remaining parameters of the line profiles.

Considering the results presented in Table 1 we can conclude that the error σ_B of the determined value $\langle B_l \rangle$ weakly depends on the measured value of $\langle B_l \rangle$ itself. At the same time this value strongly depends on the profile shape, S/N and the spectral resolving power R . The stability of the errors in $\langle B_l \rangle$ values are connected with the propagation of errors in the noise contribution to the line profile (see, e.g. Bagnulo et al. 2006).

Parameters of the model profiles are: $S/N = 500$, $R = 45000$, and $\sigma_w = 80$ km/s. From the analysis of the data presented in Table 1 we can conclude that the standard deviations for the the MIM are 30% larger than for the MDM. It can be due to the multiplier w in the expression for the first moment of the Stokes parameter V in the Eq. (2). The error in the Stokes parameter V grows in the line wings, where the values of w are large. The contribution of these regions is enhanced when we multiply the value of V by w . The difference between the values of $\langle B_l \rangle$ obtained for the MDM and the MIM, respectively, gives us the estimation of the accuracy of the magnetic field values.

3 Analysis of the multiline spectra

In this paper the multiple line spectra is treated by the same way as single lines using the *line addition* approximation. Suppose that we obtain N spectra for studied star and in each of them we select m_i unblended spectral lines for the magnetic field determination, where $i = 1, 2, \dots, N$. The full time interval ΔT when all analyzed spectra are obtained, must satisfy the condition $\Delta T < \gamma P_{\text{rot}}$, where P_{rot} is the stellar rotation period and the parameter $\gamma \leq 0.2$,

The smoothed Stokes parameter \mathcal{V} averaged over all lines in the individual spectra and over all spectra is determined by the formula:

$$\mathcal{V} = \mathcal{V}(w, S) = \frac{\sum_{i=1}^N \omega_i \sum_{k=1}^{m_i} g_{i,k} V_{i,k}(w, S)}{\sum_{i=1}^N \omega_i \sum_{k=1}^{m_i} g_{i,k}} = \frac{\sum_{i=1}^N \omega_i V_i^{\text{sp}}(w, S)}{\sum_{i=1}^N \omega_i}. \quad (17)$$

Here the value of $V_{i,k}(w, S)$ is the smoothed Stokes parameter V for the line k in spectra with the number i . The value

of $V_{i,k}(w, S)$ is determined by Eq. (12), $V_i^{\text{SP}}(w, S)$ is the Stokes parameter V averaged over all lines in the spectra with number i , ω_i is the statistical weight of the i -th spectra and $g_{i,k}$ is the statistical weight of the line k in the i -th spectra. The summation in Eq. (17) is performed over all analyzed spectra and all selected lines.

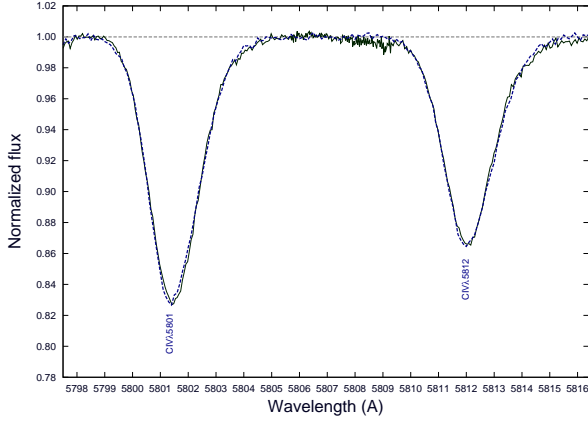


Fig. 4 The line profiles of the CIV λ 5801, 5812 Å doublet in the model spectra (thick dashed line) in a comparison with those for spectra of λ Ori A (Kholtygin et al. 2003, thin solid line). The parameters of the model spectra are given in the Table 2.

For the statistical weights of i -th spectrum one can use the expression $\omega_i \propto (S/N)_i^2$, where $(S/N)_i$ is the mean signal-to-noise ratio for the analyzed spectral region in the spectra with number i . At the same time the value of the statistical weight of the k -th line in the i -th spectra can be evaluated via the formula $g_{i,k} \propto Z_0 g_{\text{eff}} (\lambda_0^k)^2$, where Z_0 , λ_0 and g_{eff} are the central depth, effective Lande factor and the central wavelength of the line i in the spectra with a number k , respectively. The smoothed parameter $\mathcal{J}(w, S)$ in the multiline approach can be derived in the same way as the smoothed Stokes parameter \mathcal{V} in Eq. (17) from the partial values of $J_{i,k}(w, S)$. Finally the mean longitudinal magnetic field \mathcal{B}_l can be determined via the following relation:

$$\mathcal{V}(w, S) = \mathcal{B}_l \times \mathcal{J}(w, S), \quad (18)$$

where \mathcal{B}_l stands for the mean longitudinal magnetic field in the multiline approach. Eq. (18) can be used to find \mathcal{B}_l both by the MDM and by the MIM. In the last case we calculate the first moment from left and right sides of the Eq. (18). Then

$$\begin{aligned} \mathcal{M}_V &= \int_{-\Delta w}^{\Delta w} w \mathcal{V}(w, S) dw = \\ &= \mathcal{B}_l \times \int_{-\Delta w}^{\Delta w} w \mathcal{J}(w, S) dw = \mathcal{B}_l \mathcal{M}_J. \end{aligned} \quad (19)$$

The limits of integration in Eq. (19) are determined by the same manner as in Eq. (2).

The described technique for the determination of the stellar longitudinal magnetic field can be used for an arbitrary number of the polarization spectra of different quality. Moreover the spectra can be located in the different spectral regions and have an arbitrary number of lines.

To illustrate the application of the modified methods of the magnetic field measurements for multiline spectra using Eqs. (18)-(19) we simulate the model stellar spectrum in the wavelength region $\lambda\lambda$ 4000 – 6000 Å. The model spectra was created so that to be maximally close to the spectra of O8 III star λ Ori A obtained with the 1-m telescope of the Special Astrophysical observatory, Rusia (Kholtygin et al. 2003). ■

For the better approach to the line profiles in the spectrum of λ Ori A we use the normalized generalized Gaussian profile for the line shapes of the left polarized component of the lines:

$$\begin{cases} I_L^{\text{mod}}(w) = I_c + \\ Z_0 e^{-\frac{1}{2} \left(\frac{w - \Delta w_B}{\sigma_w^\alpha} \right)^\alpha} + N(0, s_N), & w < 0, \\ Z_0 e^{-\frac{1}{2} \left(\frac{w - \Delta w_B}{\sigma_w^\beta} \right)^\beta} + N(0, s_N), & w \geq 0, \end{cases} \quad (20)$$

Table 2 Parameters of lines in the model spectra of the star λ Ori A in the interval $\lambda\lambda$ 4000 – 6000 Å

Line Name	λ_{lab} (Å)	g_{eff}	Z_0	α	σ_w^α (km/s)	β	σ_w^β (km/s)
H δ	4101.737	1.00	-0.355	1.6	90	2.15	114
HeII4200	4199.87	1.06	-0.121	1.7	60	1.8	65
H γ	4340.468	1.00	-0.332	1.6	92	2.1	85
HeII4471	4471.479	1.17	-0.315	1.7	49	1.9	53
HeII4542	4541.591	1.06	-0.162	1.6	58	2.0	62
HeII4686	4685.682	1.07	-0.201	1.8	53	2.2	78
HeII4713	4713.146	1.25	-0.123	2.0	37	2.0	43
H β	4861.332	1.00	-0.352	1.8	116	2.2	94
HeII4921	4921.931	1.00	-0.164	1.7	47	1.8	43
HeI5016	5015.678	1.00	-0.140	1.8	44	2.0	43
HeII5411	5411.521	1.06	-0.207	1.7	58	2.0	66
OIII5592	5592.37	1.00	-0.155	2.0	44	1.9	40
CIV5801	5801.33	1.33	-0.173	1.8	37	1.9	52
CIV5812	5811.98	1.17	-0.136	1.8	40	1.8	50
HeI5876	5875.966	1.17	-0.375	2.6	70	1.5	35

The right polarized component can be also written using the Eq. (20), but replacing $-\Delta w_B$ by $+\Delta w_B$. The parameters α , σ_w^α and β , σ_w^β describing the line shape for the violet and red parts of the line profile can differ. All the other parameters are the same as used in the Eq. (15).

We fit the line profiles of 15 isolated lines in spectra of λ Ori A in the range $\lambda\lambda$ 4000 – 6000 Å. The list of the fitted lines is presented in the 1st column of Table 2. The laboratory wavelengths λ_{lab} listed in the 2nd column, were taken from the catalogue by Reader & Corliss (1980). The effective Landé factors were computed through the classical formulas for LS-coupling (e.g., Mathys & Stenflo 1986). The

fitting parameters Z_0 , α , σ_w^α , β and σ_w^β of all 15 lines are given in 4th - 8th columns respectively. The quality of the fit is quite good as it shown in Fig. 4.

Three model stellar spectra with the input magnetic field value $B_{\text{inp}} = 500$ G were generated for the values of $S/N = 500, 750$ and 1000 . The line parameters were taken from Table 2. After applying Eqs. (18)-(19) the mean value of $B_l = 512 \pm 14$ G for MDM and $B_l = 498 \pm 15$ G for MIM were obtained. These values differ from the input value by less than one standard deviation.

3.1 Magnetic field measurements for spectra with low signal-to-noise ratio

As it was mentioned above, the proposed methods seem to be the most effective for spectra of hot stars with broad lines and low S/N . Consider the model spectra described in the previous section in the region $\lambda\lambda 4000 - 6000 \text{ \AA}$ with lines, which are given in Table 2. Further we assume the line profile width $\sigma_w = 250$ km/s and the input value of $B_{\text{inp}} = 1$ kG, which is typical for star with the dipole field and the polar field value $B_p = 4 - 5$ kG. We also assume the relatively small spectral resolving power $R = 15000$.

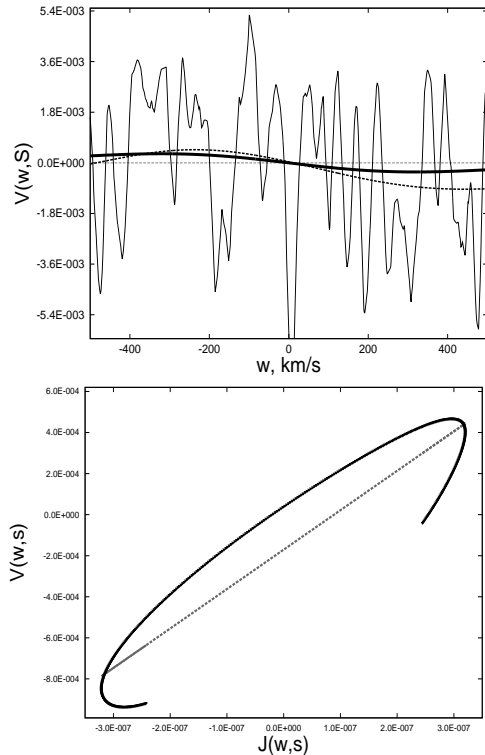


Fig. 5 Top panel: the unsmoothed Stokes parameters $V(w)$ for model spectra with lines given in Table 2 for $\sigma_w = 250$ km/s, $S/N = 300$, $R = 15000$ (thin solid line) and the smoothed Stokes parameters $V(w, S)$ for the scale parameter $S = 200$ km/s (dashed line) in a comparison with the Stokes parameters $V(w, S)$ for the same spectra, but with the zero noise contribution (thick solid line). Bottom panel: the $V(w, S)$ vs. $J(w, S)$ dependence (filled triangles) and its linear fit (dashed line).

Our calculations show that even for low $S/N \approx 300$, the longitudinal magnetic field of about of ~ 1 kG can be detected. The procedure of the field detection for the value of $S/N = 300$ is illustrated in Fig. 5. The determined values of $\langle B_l \rangle = 1203 \pm 190$ G for the MDM and 1099 ± 105 G for the MIM are in agreement at 2σ level with the input value of $B_{\text{inp}} = 1000$ G. Spectra of such quality can be obtained not only for galactic OB and WR stars but also for the stars of similar types in the Magellanic clouds and galaxies M31 and M33. It means that it is possibly to inspect the nearest galaxies for the presence of the magnetic early-type stars.

3.2 A comparison of integral and modified integral methods

To test the efficiency of the proposed modified versions of integral method of the magnetic field measurement we consider the model spectrum in the region $\lambda\lambda 4000-6000 \text{ \AA}$ using lines which are given in Table 2 and with the line widths which are the same as in the spectra of λ Ori A, as it described in the section 3. We fix the $S/N = 400$ and the spectral resolving power $R = 60000$ and compare the values of the measured magnetic field for different input values of B_{inp} obtained with the standard IM using Eq. (2) and by the MIM.

Table 3 A comparison of the input model magnetic field values B_{inp} with averaged over all lines values $\langle B_l \rangle$ obtained by IM and MIM together with the corresponding σ_B value of the scale parameter $S = 40$ km/s

B_{inp}, G	IM			MIM ^a		
	$\langle B_l \rangle, \text{G}$	$\bar{\sigma}_B, \text{G}$	σ_B	$\langle B_l \rangle, \text{G}$	$\bar{\sigma}_B, \text{G}$	σ_B
500	891	480	550	706	244	125
1000	803	588	666	913	193	176
2000	2718	972	550	2223	226	144
4000	4448	727	517	4195	270	161
8000	7291	879	589	8018	183	181

The comparison of the results obtained with the IM and the MIM is presented in Table 3. In the first column of the table we give the input model magnetic field B_{inp} , in the 2nd and 3rd columns we present the magnetic fields $\langle B_l \rangle$, which are determined by the IM from the analysis of the model spectra and the corresponding *rms* errors $\bar{\sigma}_B$. We use the standard formulas (Brandt 1970):

$$\begin{aligned} \overline{\langle B_l \rangle} &= \frac{1}{n} \sum_{i=1}^n \langle B_l \rangle_i, \\ \bar{\sigma}_B^2 &= \frac{1}{n-1} \sum_{i=1}^n \left(\langle B_l \rangle_i - \overline{\langle B_l \rangle} \right)^2. \end{aligned} \quad (21)$$

Here $\overline{\langle B_l \rangle}_i$ is the mean longitudinal magnetic field derived from the analysis of the line number i , where $n = 15$ lines were used to determine the magnetic field. In the 4th column

the real error σ_B derived from the distribution function for $\langle B_l \rangle$ (see subsection 2.6). Last three columns give the same values as those, given in the 2nd, 3rd and 4th columns, but for the MIM. It is clear that the MIM method gives more exact values of measured fields (at least for the model spectra) and smaller errors of the field determination.

The errors $\bar{\sigma}_B$, which are given in Table 3 are larger than the real error σ_B derived from the distribution function for $\langle B_l \rangle$ (see subsection 2.6).

But even if we use the error $\bar{\sigma}_B$ instead of σ_B , the moderate fields can be easily detected by the MIM at the $3\bar{\sigma}_B$ level for $B_{\text{inp}} > 500$ G. The large scattering of the values of $\bar{\sigma}_B$ in the Table 3 is connected with the relatively low S/N value.

It should be concluded that the proposed MIM of the magnetic field determination works better for low S/N polarized spectra comparing to the more simple IM. Our calculations show that the same conclusion is also valid for DM and MDM methods.

4 Application to Archival Observations

To test the efficiency of the proposed method for determination of the stellar magnetic field we apply it to study the magnetic field strength of two well known magnetic stars α^2 CVn, θ^1 Ori C and AO star HD 92207 with recently measured magnetic fields.

4.1 α^2 CVn

The chemically peculiar Ap star α^2 CVn (HD 112413) of the spectral class A0 is often used as the magnetic field standard. The effective temperature of the star is equal to 11600 ± 500 K (Kochukhov & Wade 2010), its luminosity $\approx 10^2 L_\odot$ and the rotation velocity $V \sin i = 18$ km/s (Kochukhov et al. 2002). To test our methods of the magnetic field determination we used the polarization spectra of α^2 CVn obtained on February 2, 2009 at the 6-meter telescope of the Russian Special Astrophysical observatory by Chountonov & Rusomarov (2010). Kochukhov & Wade (2010) obtained the parameters of the stellar magnetic field of α^2 CVn in the context of the oblique rotator model (Preston 1967) from the measurements of the magnetic field on the Balmer lines.

The rotation phase ϕ at the time T can be calculated via the formula $\phi = (T - T_0)/P_{\text{rot}}$, where the rotation period $P_{\text{rot}} = 5^d.46939$ (Farnsworth 1932). Using this relation and the Julian dates of the observations we compute the rotation phase $\phi = 0.138$ at the mean time of observations of α^2 CVn. For this phase the value of the longitudinal magnetic field calculated from the magnetic field phase curve by Kochukhov & Wade (2010) is $\langle B_l \rangle = -890$ G.

In Table 4 we compare the listed in the 2nd column the mean longitudinal magnetic field $\langle B_l \rangle$ values obtained via the standard relation Eq. (1) of the differential method, with those determined by the MDM and the MIM using Eqs. (12) and (14) for hydrogen lines (3rd and 4th columns). The $\langle B_l \rangle$

Table 4 Results of the magnetic field measurements (in G) for α^2 CVn for hydrogen lines by DM using Eq. (1), by MDM and MIM for $S = 40$ km/s and obtained from the phase given by Kochukhov & Wade (2010)

Line	DM ^a	MDM	MIM	Phase curve ^c
H $_{\gamma}$	-1419 ± 108	-950 ± 59	-1161 ± 51	-
H $_{\beta}$	-662 ± 81	-624 ± 25	-706 ± 64	-
H-lines	-971 ± 68	-787 ± 32	-933 ± 41	-890

values, which are determined in the different approaches are in good agreement. The detected longitudinal magnetic field strengths are also close to the value -890 G, obtained from the phase curve by Kochukhov & Wade (2010).

4.2 θ^1 Ori C and HD 92207

We also apply our modified methods of the magnetic field measurement also to the star θ^1 Ori C, which was the first O-type star with the detected magnetic field varying with the rotation period of 15.4 days (Donati et al. 2002). To determine the mean longitudinal magnetic field $\langle B_l \rangle$ we use the Stokes I and V profiles obtained by Hubrig et al. (2008) for twelve observations of θ^1 Ori C distributed over the rotational period. The observations were carried out in 2006 in service mode at the European Southern Observatory with FORS 1 mounted on the 8-m Kueyen telescope of the VLT with GRISM 600R in the wavelength range $5240 - 7380$ Å. The narrowest slit width of $0''.4$ was used to obtain a spectral resolving power of $R \sim 3000$ with GRISM 600R. The measurements were reduced in the same manner as by Hubrig et al. (2008). We used the measurements to determine the magnetic field by the MDM and the MIM.

We compare the mean $\langle B_l \rangle$ values for θ^1 Ori C obtained by us with those found by other authors. and conclude that our measurements are in a good agreement with the results by Hubrig et al. (2008), Wade et al. (2006) and Petit et al. (2008). The largest discrepancy between the measurements obtained by Hubrig et al. (2008) and by us occurs only for MJD=54182.048 at the rotation phase 0.8777. Our calculations give the values 455 ± 230 G and 421 ± 198 G for the MDM and the MIM respectively, while Hubrig et al. (2008) report the value 84 ± 54 G. But even in this case the data presented in the present paper is consistent with results published by Hubrig et al. (2008) within 2σ interval.

According to Przybilla & Nieva (2011), the abundances ratio $N/C > 0.8$ in B-type mainsequence stars indicate their possible magnetic nature. The recent determination of the atmospheric elemental abundances for the visually brightest early A0 supergiant HD 92207 (Przybilla et al. 2006) indicates a modest enrichment of nitrogen with the N/C abundance ratio of 0.83. It means that this star is a good target for searching of the magnetic field in early A-type supergiants.

The magnetic field measurements for this star were based on spectropolarimetric observations fulfilled during 2011 and 2012 with the multi-mode instrument FORS 2 installed at the 8-m Antu telescope of the VLT and were reported by Hubrig et al. (2012). The authors reported on the detection of the longitudinal magnetic field of HD 92207 at a significance level of more than 3σ for dates $MJD = 55\,688.168$ and $MJD = 55\,936.341$.

We use the observations of HD 92207 for this dates to test our modified methods of the magnetic field measurements. The determined by us values of $\langle B_l \rangle$ are given in Table 5. In the first column of the table the dates of observations is presented. In the 2nd column the line sets which are used for the field determinations are pointed. The set [all] includes all lines which can be used for the field determinations, while the set [hyd] contains only hydrogen lines. Results of the field determinations by Hubrig et al. (2012) are presented in the 3rd column. In 4th and 5th columns the field values obtained by MDM and MIM are given. Analysing the Table 5 one can conclude that both MDM and MIM fields values are in a good agreement with those given by Hubrig et al. (2012).

Table 5 Results of the mean effective magnetic field $\langle B_l \rangle$ measurements (in G) for HD 92207 using FORS 2 observations by DM (Hubrig et al. 2012) and by MDM and MIM for $S = 30$ km/s

MJD	Line sets	DM	MDM	MIM
55 688.168	[all]	-384 ± 42	-473 ± 83	-477 ± 100
	[hyd]	-402 ± 52	-530 ± 68	-527 ± 89
55 936.341	[all]	145 ± 38	247 ± 46	250 ± 77
	[hyd]	157 ± 51	246 ± 45	247 ± 58

Resuming the results of this section we can conclude that proposed in the present paper MDM and MIM methods give a good results for simple fields. They also let to reach the acceptable results for the complex structure of the magnetic fields which are close to those obtained by other methods.

5 Conclusion

In the present paper the modified methods of the stellar magnetic fields measurement are described. This method is based on the application of the wavelet transform with DOG-wavelets to the integral line profiles and the smoothing with the Gaussian function to the Stokes parameter V . The proposed method can be used both for isolated lines in the stellar spectra and for the wide spectral regions including arbitrary numbers of the unblended lines, and also for a number of stellar spectra with close rotation phases.

The application of the proposed method to the model stellar spectra shows that this method is most efficient for stellar spectra having unblended lines with line widths larger than $30 - 40$ km/s. The main advantage of the method is the effective suppression of the noise contribution both to the line profile in integral light and in the Stokes parameter V . Moreover, this method can be tuned for the individual spectra by the selection of the optimal value of the scale S . The proposed in the present paper MDM and MIM methods are valid for simple, large-scale fields and using them for the magnetic fields of complex structure may be less successful. We plan to investigate the efficiency both MDM and MIM methods for complex fields in following papers.

In the paper we consider only the case $k = 0$ of the smoothing the Stokes parameter V with the family of functions $\mathcal{G}_k(x/S)$, which are determined by Eq. (11). Accepting the value of $k = 1$ we obtain the gaussian-like form of the smoothed function $V_1(w, S)$. It means that the case $k = 1$ may be more convenient for the analysis of the polarized spectra with the overlapping lines. The cases $k > 1$ probably are not very suitable for such analysis due to the complex structure of the DOG-wavelets with indexes $k \geq 2$. The proposed method for the case $k = 1$ will be developed in the future publications.

Acknowledgements. I am grateful to the referee for his valuable comments. I thank to G. A. Chountonov for the presentation the polarized spectra of α^2 CVn and N. Rusomarov for processing this spectra with the MIDAS package. I am also grateful to S. Hubrig for giving a possibility to use her spectropolarimetric observations of θ^1 Ori C and HD 92207 to test the methods. This work was supported by a Saint-Petersburg University project 6.38.73.2011.

References

- Babcock, H.W.: 1947, ApJ 105, 105
- Bagnulo, S., Szeifert, T., Wade, G.A., Landstreet, J.D., Mathys G.: 2002, A&A 389, 191
- Bagnulo, S., Landstreet, J.D., Mason, E., Andretta, V., Silaj, J., Wade, G.A.: 2006, A&A 450, 777
- Brandt, S.: 1970, Statistical and Computational methods in data analysis, North Holland Publ. Comp., Amsterdam - London
- Bychkov, V.D., Bychkova, L.V. Madej, J.: 2009 MNRAS 394, 1338
- Chountonov, G.A., Rusomarov, N.: 2011 private communication
- Farnsworth, G.: 1932 ApJ 76, 313.
- Hubrig, S., Briquet, M., Schöller, M., De Cat, P., Mathys, G., Aerts C.: 2006 MNRAS 369, L61
- Hubrig, S., Schöller, M., Schnerr, R.S., Gonzalez, J.F., Ignace, R., Henrichs, H.F.: 2008 A&A 490, 793
- Hubrig, S., Schöller, M., Kholtygin, A.F., Gonzalez, J.F., Kharchenko, N.V., Steffen M.: 2012 A&A 546, L6
- Donati, J.-F., Semel, M., Carter, B.D., Rees, D.E., Cameron, A.C.: 1997 MNRAS 291, 658
- Donati, J.-F., Babel, J., Harries, T.J., Howarth, I.D., Petit, P., Semel, M.: 2002 MNRAS 333, 55
- Kholtygin, A.F., Monin, D.N., Surkov, A.E., Fabrika, S.N.: 2003 Astronomy Letters, 29, 175
- Kholtygin, A.F., Burlakova, T.E., Fabrika, S.N., Valyavin, G.G., Yushkin, M.V.: 2006 Astronomy Reports 50, 887

- Kholtygin, A.F., Sudnik, N.P., Burlakova, T.E., Valyavin, G.G.: 2011a *Astronomy Reports* 55, 1105
- Kholtygin, A.F., Fabrika, S.N., Rusomarov, N., Hamann, W.-R., Kudryavtsev, D.O., Oskinova, L.M., Chountonov, G.A.: 2011b AN 332, 1008
- Kochukhov, O., Piskunov, N., Ilyin, I., Ilyina, S., Tuominen, I.: 2002 *A&A* 389, 420
- Kochukhov, O., Bagnulo, S., Wade, G.A., Piskunov, N., Landstreet, J.D., Petit, P., Sigut T.A.A.: 2004 *A&A* 414, 613
- Kochukhov, O., Makaganiuk, V., Piskunov, N.: 2010 *A&A* 524, A5
- Kochukhov, O., Wade, G. A.: 2010 *A&A* 513, A13
- Landstreet, J.D.: 1982 *A&A* 258, 639
- Mathys, G., Stenflo J.O.: 1986 *A&A* 168, 184
- Mathys, G.: 1995 *A&A* 293, 746
- Mathys, G., Hubrig S.: 1997 *A&A Suppl. Ser.* 124, 475
- De Moortel, I., Munday, S.A., Hood, A.W.: 2004 *Sol. Phys.* 222, 203
- Petit, V., Wade, G.A., Drissen, L., Montmerle, T., Alecian, E.: 2008 *MNRAS*. 387, L23
- Petit, P., Lignières, F., Wade, G. A., Aurière, M., Böhm, T., Bagnulo, S. Dintrans, B., Fumel, A., Grunhut, J., Lanoux, J., Morgenthaler, A., Van Grootel, V.: 2010 *A&A* 523, A41
- Preston, G.W.: 1967, *ApJ* 150, 547
- Przybilla, N., Butler, K., Becker, S.R., Kudritzki, R.P.: 2006 *A&A* 445, 1099
- Przybilla, N., Nieva, M. F.: 2011 *Proc. IAU Symp.* 272, 26
- Ramirez Velez, J.C., Semel, M., Stift, M., Martinez Gonzalez, M.J., Petit, P., Dunstone, N.: 2011 *A&A* 511, A6
- Semel, M. 1989 *A&A* 225, 456
- Semel, M., Li, J.: 1996 *Sol. Phys.* 164, 417
- Wade, G.A., Fullerton, A.W., Donati J.-F., Landstreet, J.D., Petit, P., Strasser, S.: 2006 *A&A* 451, 195
- Reader, J., Corliss, C.H.: 1980, *Wavelengths and Transition Probabilities for Atoms And Atomic Ions*, NSRDS-NBS 68

